

Attracted Diffusion-Limited Aggregation

S. H. Ebrahimnazhad Rahbari^{1,2*} and A. A. Saberi^{3,4†}

¹*Plasma and Condensed Matter Computational Lab,
Azarbayjan University of Tarbiat Moallam, Tabriz, Iran.*

²*Max-Planck Institute for Dynamics and Self-Organization,
Department of Complex Fluids, 37073 Göttingen, Germany*

³*Department of Physics, University of Tehran, Post Office Box 14395-547, Tehran, Iran*

⁴*Institut für Theoretische Physik, Universität zu Köln, Zùlpicher Str. 77, 50937 Köln, Germany*

(Dated: November 27, 2024)

In this paper, we present results of extensive Monte Carlo simulations of diffusion-limited aggregation (DLA) with a seed placed on an attractive plane as a simple model in connection with the electrical double layers. We compute the fractal dimension of the aggregated patterns as a function of the attraction strength α . For the patterns grown in both two and three dimensions, the fractal dimension shows a significant dependence on the attraction strength for small values of α , and approaches to that of the ordinary two-dimensional (2D) DLA in the limit of large α . For non-attracting case with $\alpha = 1$, our results in three dimensions reproduce the patterns of 3D ordinary DLA, while in two dimensions our model leads to formation of a compact cluster with dimension two. For intermediate α , the 3D clusters have *quasi*-2D structure with a fractal dimension very close to that of the ordinary 2D-DLA. This allows one to control morphology of a growing cluster by tuning a single external parameter α .

PACS numbers: 61.43.Hv, 47.57.eb, 66.10.C-, 68.43.Jk, 82.40.Ck

I. INTRODUCTION

By immersing an object with large surface-area-to-volume ratio into an ionic solution, it is surrounded by a double layer of electrical charge that significantly influences its surface behavior [1, 2]. Electrical attraction of free ions with thermal motion in the fluid by the surface charge, forms a second layer, known as diffuse layer, that shields out the Coulomb potential of the surface layer and makes the whole structure electrically neutral. Applications of double layer range from plasma physics [3], to colloidal science [4], and micro- and nano-fluidics [5].

As a simple theoretical model for the formation of a diffuse layer in a special case, we implement extensive Monte Carlo simulations for attracted random walks (ARW) introduced by Saberi [6], in order to study the formation of ionic aggregates on and near an infinite plane located at $z = 0$. An infinite surface charge exerts a uniform constant electric force on the free ionic particles in the fluid. It is, therefore, reasonable to consider an infinite attractive plane of uniform attraction strength α which acts on a free random walker launched from a point far from the attractive plane. An ionic *seed* is located at the center of the infinite plane. Upon contacting, the free ionic random walker sticks irreversibly to the cluster due to an absorbing bond introduced between the ionic particles.

The diffusion of an attracted Brownian particle of mass m in a fluid may be given by the following Langevin equation

tion

$$m\ddot{z} + \gamma\dot{z} + \alpha \text{sgn}(z) = \xi(t), \quad (1)$$

where the second term denotes a viscous-like friction force with drag γ , the third term stands for an attraction force of strength α exerted by an infinite plane at $z = 0$, and $\xi(t)$ is a Gaussian white noise characterized by

$$\langle \xi(t) \rangle = 0, \quad \langle \xi(t)\xi(t') \rangle = 2D\delta(t - t'), \quad (2)$$

with D being the diffusion coefficient.

While such a Langevin-like equation (1), to our best knowledge, has not been studied previously, we implement such a process to produce a diffusion-limited aggregated pattern on an attractive plane and investigate its fractal properties in terms of the strength of attraction α . We apply two different mechanisms in our model to produce the aggregates. First, the aggregates are let to grow freely in three dimensions, *i.e.*, the 3D-ARW sticks to the aggregate upon touching the cluster giving rise to the formation of a 3D pattern. Second, the aggregates are restricted to only grow within the attractive plane, *i.e.*, the 3D-ARW sticks to the aggregate only if it touches the cluster within the attractive plane, which leads to the formation of a 2D pattern.

Our results indicate that for small α , the fractal dimensions for both cases depend significantly on the strength of attraction, and in the limit of large α , they converge to the fractal dimension of the ordinary two-dimensional (2D) diffusion-limited aggregation (DLA). This rapid convergence, however, implies the formation of a *quasi*-2D pattern for a 3D aggregate for intermediate values of α . Furthermore, for the two limiting cases, *i.e.*, $\alpha = 1$ and $\alpha \rightarrow \infty$, our model reproduces the results of the ordinary DLA. Loosely speaking, for $\alpha = 1$, the 3D-ARW is identical to the ordinary 3D-RW and thus our model generates

*Electronic address: sebrahi1@gwdg.de

†Electronic address: ab.saberi@ut.ac.ir

the same patterns as the ordinary DLA in three dimensions. In the limit of $\alpha \rightarrow \infty$, the 3D-ARW can only move within the attractive plane and is indeed identical to the 2D-RW and thus, in both cases, the patterns of the ordinary DLA in two dimensions are reproduced. The only difference is for $\alpha = 1$ in two dimensions, where our model gives a new class of aggregates which are compact clusters with dimension two.

The ordinary DLA, known also as a Brownian tree, was originally introduced by Witten and Sander [7] to model the aggregates of metal particles formed by adhesive contact in low concentration limit. This model is shown to describe many pattern formation processes including dielectric breakdown [8], electrochemical deposition [9, 10], viscous fingering and Laplacian growth [11]. According to this model, the walker does a random walk process initiated from infinity like as described above in our model but without experiencing any external force. Many of its fractal properties have then been reported from various simulations done both in real and mathematical plane (see for example [12] and references therein).

This study uncovers a new insight into various related phenomena with a discrete time lattice walk [13, 14], relaxation phenomena [15], exciton trapping [16] and diffusion-limited reactions [14, 17].

II. ATTRACTED DIFFUSION-LIMITED AGGREGATION (ADLA)–DETAILS OF SIMULATION

In this section, we investigate aggregation of ARWs on and near an attractive plane based on the algorithm proposed in [7] for ordinary DLA clusters, accompanied by the details of simulations. For M being the total number of particles, or equivalently the cluster *mass*, the simulation box is considered to be a cube of size $L_x = L_y = 20\sqrt{M}$ and $L_z = 60\sqrt{M}$. The box is divided into a regular lattice of $L_x \times L_y \times L_z$ cubic cells of unit size. Periodic boundary conditions are applied along all three directions. The attractive plane is a horizontal plane at $z = \frac{L_z}{2} := 0$ whose bottom-left corner is taken as origin of the coordinate system. We store information of each lattice site by an integer in the computer. Accordingly, the total memory to be occupied by the lattice will be equal to $4L_xL_yL_z \approx 10^5 M^{3/2}$ Bytes. One sees that as the total number of particles M increases, the total memory grows rapidly and for large M the total memory becomes so huge that can not be handled by conventional computers. In order to prevent excessive memory usage, we apply different restrictions to our algorithm to reduce the memory. These tricks will separately be discussed for both 2D and 3D clusters in Sec. II A and Sec. II B respectively.

First, let us briefly review the probabilities governing the movement of an ARW [6]. For the random walker at $z \neq 0$, there are six directions which can be chosen by the walker. One is that points towards the plane whose prob-

ability is set to αp , where $\alpha > 1$ is strength of the attraction. For the five directions being left, the corresponding probability of each link is equally set to p , providing $p = \frac{1}{\alpha+5}$. For the random walker at $z = 0$, there are two directions perpendicular to the plane whose probability is p' , and four directions on the plane each of which with the probability $\alpha p'$, such that $p' = \frac{1}{4\alpha+2}$. This setting of probabilities guaranties that the walker likes to ramble on and around the attractive plane.

It is well known that formation of DLAs is dominated by diffusive motion rather than the convective one. Therefore, the walker must start to move far enough away from the attractive plane. Once a seed particle is settled on the attractive plane, a random walker is introduced on a random lateral position at height $z_0 = 15\sqrt{M}$, and moves according to the probabilities having been de-

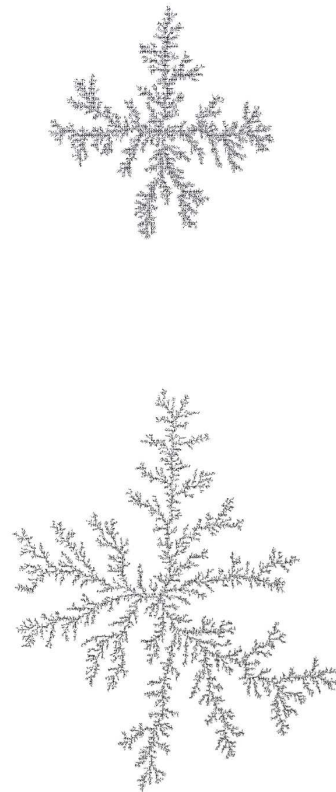


FIG. 1: Snapshots of the growing clusters for $\alpha = 1.2$ (Top), and $\alpha = 10$ (Bottom), with the same number of particles $M = 10^5$. The radius of gyration is $R_G = 251.5$ and $R_G = 410.54$ for the top and bottom figures, respectively. Distance from camera is the same for both clusters. One sees that the gyration radius of the clusters, R_G , increases with the attraction strength α . Moreover, for small α the cluster has fat arms, while for larger α the chains are much elongated and delicate. The pictures are rendered by the *Povray* software.

scribed above. The walker keeps moving until it sticks to the seed. Following that, a new random walker is introduced at $z_0 = 15\sqrt{M}$ from a random lateral position, and is let to move until it sticks to one of those particles being frozen. This procedure is applied until the desired number of the particles in the cluster, *i.e.*, M , is reached. For the growth of 2D and 3D structures, we implement different additional rules that will be discussed in Sec. II A and Sec. II B.

A. 2D structures

2D structures are formed based on a *land-escape* procedure. When a particle is either at $z = +1$ or $z = -1$, it may *land* on the plane if its shadow on the plane is not occupied, otherwise it must *escape* to one of the five remaining directions with equal probabilities. Once the particle has landed on the plane, it will diffuse according to the aforementioned rules until it finds at least one frozen particle on its neighborhood and gets stuck to that point. It should be stressed out that according to the probabilities governing the motion of the ARWs, there still exists a probability for the walker to break from the plane and fly back into the space.

From our numerical experiments, we empirically found that the radial distance of the farthest particles from the seed never exceeds $r = 8\sqrt{M}$ limit. We used this fact to accelerate our simulation runs, in a way that the attractive plane is being divided into two distinct regions, the inner region where the cluster forms, and, the outer region where the random walker moves freely with no need for exploring a possible occupied nearest-neighbor site. We employed this fact in our simulations and found that it considerably decreases the computational effort.

In figure 1, two snapshots of the growing clusters on the attractive plane are shown for two different strength of attraction $\alpha = 1.2$ and $\alpha = 10$, shown at the top and bottom of the figure, respectively. The cluster mass $M = 10^5$ and the distance from camera are considered to be the same for both patterns for a comparison. Both figures have a fractal structure with a rotational symmetry about the z -axis and the same number of main branches. For lower α , the particles are being condensed along the main arms giving rise to much fatter branches than for the larger α for which, the cluster has delicate chains elongated on the attractive plane with deeper fjords and sharper tips. It is also evident that the gyration radius R_G of the clusters increases with the attraction strength α . Here, the gyration radius—in units of a particle diameter—is found to be $R_G = 220.8$ and $R_G = 410.54$ for $\alpha = 1.2$ and $\alpha = 10$, respectively.

In order to get a more quantitative insight about the structure of the clusters, we compute the gyration radius R_G of different clusters grown under the same conditions but with different strength of attraction α . Figure 2 illustrates the cluster mass M as a function of the gyration radius R_G of the clusters for various α . Since the ensemble

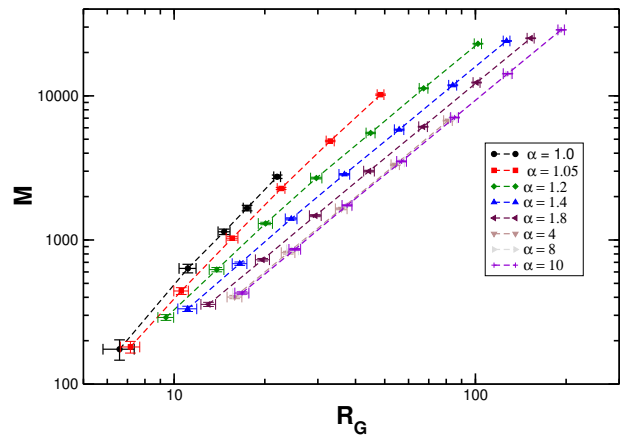


FIG. 2: Cluster mass M as a function of the radius of gyration R_G of the 2D growing clusters on the attractive plane for different values of α . For $\alpha \gtrsim 1.15$, the curves exhibit a full power-law behavior Eq. (3).

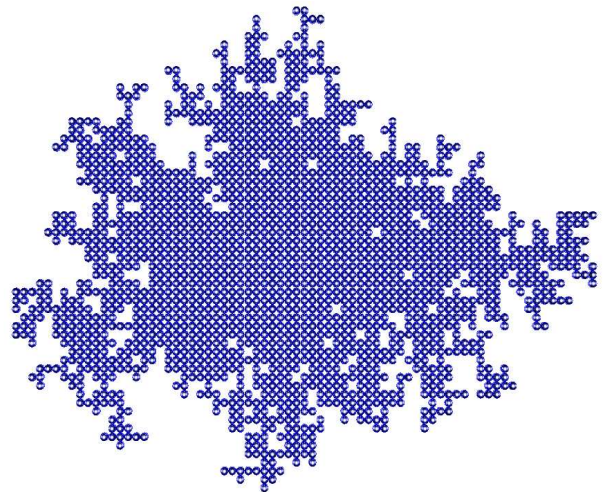


FIG. 3: A typical example of a 2D cluster grown on the attractive plane with $\alpha = 1$. The number of particles is $M = 1875$ which forms a compact cluster of dimension ≈ 2 , with gyration radius $R_g \simeq 19.62$.

averaging plays a crucial role in such computations, the averages, for each point in the Fig. 2, are taken over 90 different clusters for given values of α and M . It is well-known that the following relation is usually held for fractal patterns

$$M \propto R_G^{D_f}, \quad (3)$$

where D_f is the fractal dimension of the cluster. Our results are in accord with this power-law relation (3) for $\alpha \gtrsim 1.15$. For smaller values of α , the ARW crosses over to the ordinary 3D-RW and starts to fill in the empty regions between the branches. This leads the cluster to

being much condensed. A typical example of such a compact cluster for $\alpha = 1$ is shown in Fig. 3. Although the power-law behavior is disturbed, within our numerical accuracy, for $\alpha \rightarrow 1$, their outer perimeter may keep their fractal properties as it comes out from Fig. 3 [22]. This would be investigated in more detail in a future work.

According to our model, for $\alpha = 1$ the attraction strength is set to zero. As a principle of DLA, random walkers should initiate their motion from the infinity (far from the seed). Therefore, there is a very little chance to find a random walker, triggered at infinity, on the surface of the attractive plane. Within this small chance, again there is a very little probability to keep the particle moving on and around the plane. Once the particle lands on the plane, normally it tends to escape to infinity and hardly finds a frozen particle in its neighborhood to join to the cluster. Consequently, for 2D clusters at $\alpha = 1$ the growth rate is almost zero and we observe only clusters with small mass $500 < M < 3000$ which is not enough to examine any scaling relation. Therefore, we get a poor statistics for $\alpha = 1$ (see also Fig. 6).

B. 3D structures

In contrast to 2D structures, the growth model for 3D clusters is not restricted to the surface of the attractive plane. Instead, the random walker in this case can get stuck in any lattice site whose each of the nearest-neighbor sites is already occupied, whether or not being in the attractive plane.

In figure 4, we show some of the resulting patterns obtained by this algorithm in three dimensions. The figure shows a side view of the grown clusters consisting $M = 10^5$ particles with $\alpha = 1.2, 2$ and 10 , with $R_G = 199.6, 342.8$ and 405.9 , from top to bottom, respectively. Two different colors are chosen for the particles: the metallic (gray) color for those sitting on the attractive plane at $z = 0$, and the red (dark) color for particles sitting elsewhere with $z \neq 0$. As can be seen from the figure, the number of red (dark) particles is significantly dependent on the strength of attraction. For small α , the ARW can easily wander around and thus, it is more likely for the particle to get a chance to stick to the cluster somewhere at $z \neq 0$, while for larger α , the ARW is almost rambling on and near the attractive plane which increases the sticking probability within the plane. In the limit of $\alpha \rightarrow \infty$, the 3D-ARW falls onto the ordinary 2D-RW giving rise to the formation of ordinary DLA clusters in pure two dimensions. For $\alpha = 1$, at the other limiting side, the 3D-ARW is the same as the ordinary 3D-RW and we get back the ordinary 3D-DLA patterns.

We empirically found that for $1 < \alpha < 1.2$, the thickness of 3D clusters on either side of the attractive plane never exceeds 35 particle diameter, even for clusters of size up to $M = 10^5$. Also, for $\alpha > 1.2$, the height of the tallest tower in the cluster never reaches 10. Based

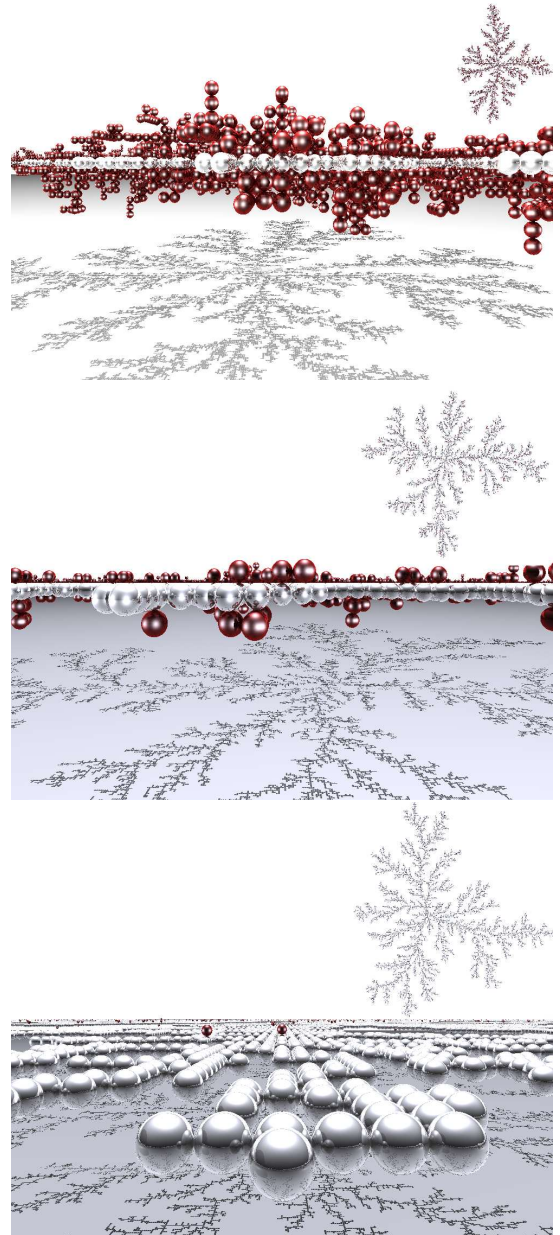


FIG. 4: Three typical examples of 3D grown clusters of number of particles $M = 10^5$. The metallic (gray) particles lie on the attractive plane, and the rest—not on the surface—are illustrated by the red (dark) color. The strength of attraction is considered to be $\alpha = 1.2, 2$ and 10 , with $R_G = 199.6, 342.8$ and 405.9 , from top to bottom, respectively. The maximum height of the towers perpendicular to the attractive plane never exceeds 10 particle diameter on either side of the attractive plane, implying the formation of *quasi*-2D clusters.

on this experimental evidence, similar to that of the 2D case, the simulation box can technically be divided into two following distinct volumes to reduce the memory. An inner volume *i.e.*, with $-35 \leq z \leq 35$ for $1 < \alpha < 1.2$, and $-10 \leq z \leq 10$ for $\alpha > 1.2$, where the cluster can form and the rest as the outer volume where the particle

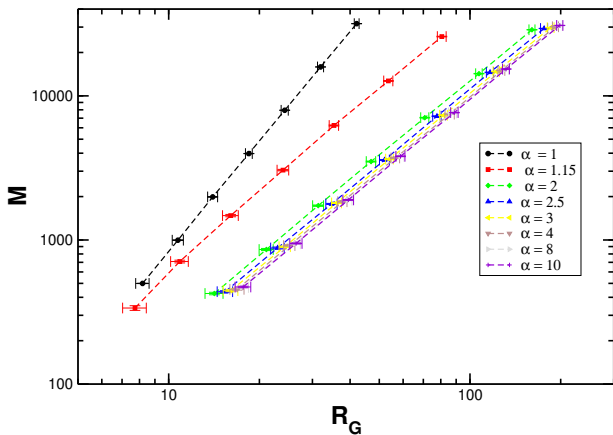


FIG. 5: Cluster mass M as a function of the radius of gyration R_G of the 3D growing clusters formed around the seed placed on the attractive plane for different values of α .

moves freely without an extra check for looking up for an occupied nearest-neighbor site. We applied this fact in the structure of our programming codes and found that it considerably speeds up the simulations.

The quantity of interest is again the gyration radius, R_G , for clusters of different mass M . Figure 5 shows our results of cluster mass for 3D clusters as a function of their gyration radius for different attraction strength α . Each point in Fig. 5 is averaged over an ensemble of 90 independently grown samples. The mass of clusters range between $500 \leq M \leq 32000$. Error-bars for both R_G and M are visible in the plot. We found a perfect scaling behavior for $\alpha \geq 2$, whereas for $1 < \alpha < 2$ our data fits to a power-law with higher uncertainty (this is also much evident from the inset of Fig. 6). One also sees that for a constant cluster mass, the gyration radius increases upon increasing the attraction strength which is due to the elongation of the growing cluster within the attractive plane. As mentioned above, the thickness d of the clusters along the z -axis never exceeds 70 particle diameter even for clusters of size up to $M = 10^5$. This implies a considerably small relative thickness, defined as $d/R_G \ll 1$, for the patterns, and thus indication of the formation of *quasi*-2D clusters. This would later be confirmed in the next section where we compute the fractal dimension of the grown patterns.

III. FRACTAL DIMENSION OF 2D AND 3D ADLA CLUSTERS

In this short section, we compute the fractal dimension of the clusters as a measure characterizing the statistical complexity of the grown fractal patterns in both two and three dimensions. The fractal dimension of the clusters can easily be calculated from the data given in Fig. 2 and Fig. 5 by examining the scaling relation (3).

In figure 6, we compile our data for the fractal dimensions of 2D and 3D clusters which are represented by the open circles (\circ) and squares (\square), respectively.

For both 2D and 3D clusters, the fractal dimension significantly depends on the strength of attraction α , especially for $\alpha < 2$. The smaller the α , the denser the clusters are. For larger α , the fractal dimensions in both cases, are less dependent on α , rapidly converging to the value $D_f \approx 1.72$ which, within the statistical errors, is almost in accord with that of the ordinary DLA clusters in two dimensions with $D_f \approx 1.71$.

As discussed before, the overall intermediate fractal behavior seems to be dominated by the two crossover limits in the statistical behavior of the underlying diffusion process *i.e.*, the crossover of the 3D-ARW to ordinary 3D-RW and 2D-RW for $\alpha = 1$ and $\alpha \rightarrow \infty$, respectively. For $\alpha = 1$, the 2D clusters have a compact structure of dimension ≈ 2 , and for the 3D clusters we obtain a fractal dimension $D_f \approx 2.53$ very close to the expected value for the ordinary 3D-DLA [19].

IV. DISCUSSION AND CONCLUSION

In conclusion, we introduced a model of aggregation based on an extension of diffusion-limited aggregation where the underlying diffusion process is a 3D Brownian motion (or, a random walk on the lattice) which is attracted by a plane with strength α . The *seed* particle is placed on the attractive plane.

In two dimensions, the fractal properties of the aggregated cluster is shown to be dependent on the attraction strength giving rise to formation of patterns with $1.71 \lesssim D_f \leq 2$. The two limiting values for the fractal dimension D_f , in the scaling region, are discussed to be governed by the crossover of the 3D-ARW to the ordinary 3D-RW for $\alpha \rightarrow 1$ from one side, and its convergence to the ordinary 2D-RW at the other side with $\alpha \rightarrow \infty$, which leads to ordinary 2D-DLA patterns of $D_f \approx 1.71$.

In three dimensions, the rotational symmetry, which is present in the ordinary 3D-DLA clusters with $\alpha = 1$, is broken by the attractive plane with $\alpha > 1$, and the model leads to formation of clusters with $1.71 \lesssim D_f \lesssim 2.53$. For intermediate α , we obtain *quasi*-2D clusters whose relative thickness, defined as the thickness of a cluster perpendicular to the attractive plane rescaled by its radius of gyration, is relatively small. Our results indicate a scaling region with $\alpha \gtrsim 2$, in which the fractal structure of the clusters can be characterized by a single fractal dimension $D_f \approx 1.72$, independent of α .

Recently, there has been a growing attention and frequent reports on the fact that morphology of self-assemblies can be controlled by tuning various physical parameters such as the packing fraction ϕ , and the attraction strength. This is specifically important for handling of soft materials and food processing. In our study, we found out that a crossover from ramified, fractal clusters to compact aggregates occur upon decreasing the attrac-

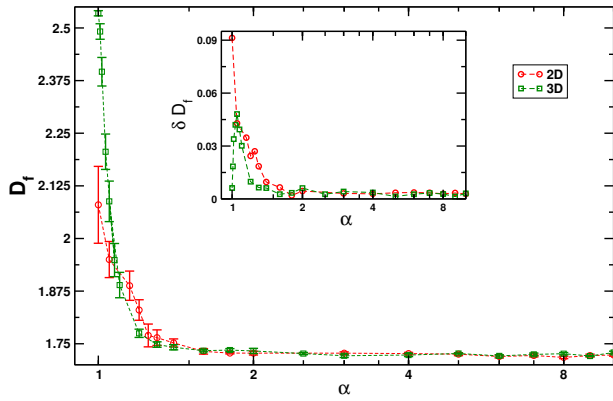


FIG. 6: The fractal dimension D_f of the attracted diffusion-limited aggregation clusters grown in two and three dimensions, represented by open circles (\circ) and squares (\square), respectively, as a function of the attraction strength α . The inset shows the corresponding error bars within which the power-law behavior Eq. (3) holds.

tion strength α at the limit of small attraction strength. For the two dimensional clusters the threshold is found to be $\alpha_c = 1.15$. As a result, in our model morphologies of the growing clusters can be controlled by tuning the attraction strength α .

In a recent study of aggregation of hard spheres [20], a similar crossover from a compact to ramified aggregation is found which in the former regime the scaling relation fails while in the latter case the scaling holds. The crossover from compact to fractal clusters happens upon increasing the packing fraction ϕ . The threshold is found to be at $\phi = 0.55$ which is very close to the

glass transition point at $\phi_g = 0.58$. Therefore, in this case, the structure of aggregations can be controlled by the packing fraction ϕ . Zhang *et.al.*, [21] report results of experiments on colloidal suspensions with short-range attraction and long-range repulsion. They show that the morphology of the clusters can be controlled by tuning either the attraction strength or the packing fraction ϕ resulting to an elongated-to-branched crossover.

These reports imply that the compact-to-ramified crossover may be considered as a universal property of aggregation of particles. Consequently, this can suggest the possibility of proposing a single phase-diagram that captures such behavior for different systems with different underlying physical processes and inter-particle interactions.

A possible future work for constructing a much more realistic model of diffusive layer may be an extension of the present model by considering a number of mobile seed particles on the attractive plane that the growth of each can be given by our implemented procedure. In that case, the growing clusters can stick together upon contacting. The results will appear elsewhere in the near future.

V. ACKNOWLEDGMENTS

We would like to thank M. Ghorbanalilu for his fruitful comments. SHER is partially supported with a fund number 218-D-3390, granted by Azarbayjan university of Tarbiat Moallem. AAS acknowledges the partial financial support by the research council of the University of Tehran, and INSF grant as well.

-
- [1] J. Lyklema, *Fundamentals of Interface and Colloid Science Vol. II: solid-liquid interface*, Academic press, London (1995).
 - [2] R. J. Hunter, *Foundations of colloid science*, Oxford University, New York (2001).
 - [3] F F Chen, *Plasma Physics* (2006).
 - [4] R J Hunter, *Foundations of Colloid Science* (1989).
 - [5] B J Kirby, *Micro- and Nanoscale Fluid Mechanics: Transport in Microfluidic Devices* (2010).
 - [6] A A Saberi, Phys. Rev. E **84**, 021113 (2011).
 - [7] T. A. Witten, Jr. and L.M. Sander, Phys. Rev. Lett. **47**, 1400 (1981).
 - [8] L. Niemeyer, L. Pietronero, and H. J. Wiesmann, Phys. Rev. Lett. **52**, 1033 (1984).
 - [9] R. M. Brady and R. C. Ball, Nature (London) **309**, 225 (1984).
 - [10] M. Matsushita, M. Sano, Y. Hayakawa, H. Honjo and Y. Sawada, Phys. Rev. Lett. **53**, 286 (1984).
 - [11] L. Paterson, Phys. Rev. Lett. **52**, 1621 (1984).
 - [12] A. A. Saberi, J. Phys.: Condens. Matter **21**, 465106 (2009); F. Mohammadi, A. A. Saberi and S. Rouhani, J. Phys.: Condens. Matter **21**, 375110 (2009); J. Phys. A: Math. Theor. **43**, 375208 (2010).
 - [13] J. Haus and K. W. Kehr, Phys. Rep. **150**, 263 (1987).
 - [14] A. Bunde and S. Havlin, *Fractal and Disordered Systems* (Springer-Verlag, Berlin, 1991).
 - [15] C. A. Condat, Phys. Rev. A **41**, 3365 (1990).
 - [16] H. B. Rosenstock, Phys. Rev. **187**, 1166 (1969).
 - [17] G. H. Weiss and R. J. Rubin, Adv. Chem. Phys. **52**, 363 (1983).
 - [18] A. A. Saberi and S. Rouhani, Phys. Rev. E **79**, 036102 (2009).
 - [19] S. Tolman and P. Meakin, Phys. Rev. A **40**, 428437 (1989).
 - [20] C. Valeriani, E. Sanz, P. N. Pusey, W. C. K. Poon, M. E. Catesb and Emanuela Zaccarellic, Soft Matter, 10.1039 (2012).
 - [21] T. H. Zhang, J. Klok, R. Hans Tromp, J. Groenewold, and W. K. Kegel, Soft matter **8**, 667 (2012).
 - [22] Similar to the compact islands appear in a 2D cross-section of a height profile in a (2+1)-dimensional Kardar-Parisi-Zhang equation [18].